THE ROLE OF ACCELERATORS IN THE NUCLEAR FUEL CYCLE

Hiroshi Takahashi
Brookhaven National Laboratory
Upton, New York 11973

BNL--43887

DE90 008823

I. INTRODUCTION

The use of neutrons produced by the medium energy proton accelerator (1Gev-3Gev) has considerable potential in reconstructing the nuclear fuel cycle. About 1.5 - 2.5 ton of fissile material can be produced annually by injecting a 450 MW proton beam directly into fertile materials. A source of neutrons, produced by a proton beam, to supply subcritical reactors could alleviate many of the safety problems associated with critical assemblies, such as positive reactivity coefficients due to coolant voiding. The transient power of the target can be swiftly controlled by controlling the power of the proton beam. Also, the use of a proton beam would allow more flexibility in the choice of fuel and structural materials which otherwise might reduce the reactivity of reactors.

There is now a plan to permanently store long-lived highly radioactive waste in a stable geologic formation such as Yucca Mountain in Death Valley. There is concern, however, that geologic formations and the climate might change over millions of years. Therefore, it may be worthwhile to study an alternative approach to store the waste that would separate the long-lived nuclei from the high-level waste by transmuting them into short-lived or non-radioactive wastes.

Studies of the incineration of actinide nuclei that have very long half-lives, such as ^{237}Np, indicate that small beam power, in the order of 15-30 MW, can incinerate the actinide produced by ten 1GWe light water reactors. Furthermore, an incinerator with 900 MW thermal power can produce 270-240 MWe

of excess electricity, as well as the 100 Kg of fissile material such as ^{233}U or ^{239}Pu when its core is surrounded with fertile material such as ^{232}Th or ^{238}U, respectively.

Because of its small capture cross-section, the incineration of ^{137}Cs, whose half-life is 30 years, at a rate of 10 times its natural decay would require a high intensity thermal neutron flux of 10^{17} n/cm^2/sec. It is difficult to create this very high thermal neutron flux, even with spallation neutrons. Yet, if the momentum spread of μ- secondary particles created by the collision of a deuteron and light element nucleus can be reduced, it is possible to make a high flux of muon-catalyzed 14 MeV fusion neutrons (10^{16} n/cm^2/sec) in a small synthesizer vessel; ^{137}Cs can be incinerated by using (n,2n) or (n,3n) reactions, which have a cross section of 1-2 barns, at the rate of 10-20 times natural decay.

This reduction of the momentum spread of the secondary particles is essential for collecting antiproton which might be used for medical and basic physical studies, and also for future space propulsion fuels.

Present accelerator technology is based on microwave technology. Laser technology, which is a rapidly advancing field, has the potential of advancing accelerator technology by achieving, for example, a high acceleration rate of 1 GeV/m. The achievement of a small beam size, in the order of 1 micron at SLAC and the rapid progress in micro-fabrication of miniature grating lattices are encouraging developments that extend the frontiers of accelerator technology which, in turn, will benefit the reactor fuel cycle.

II. THE ACCELERATOR BREEDER

The concept of using an accelerator to produce fissionable material is not new; it was proposed at an early date in the nuclear age (1950) by E. O. Lawrence and others at Berkeley.[1] To be independent of foreign sources of uranium used to make plutonium for weapons, a project was planned to produce plutonium from the low ^{235}U concentration tailings accumulating at the diffusion plant at Oak Ridge National Laboratory. Thus, the so-called MTA (Material Testing Accelerator) Project was begun. The MTA project proceeded quite far into the problems of engineering, developing, and building a prototype of an accelerator-breeder facility; the project was terminated when substantial amounts of uranium ores were discovered in the Western part of the United States.

The construction of an accelerator had begun when the MTA project ceased in 1954. Figure 1 shows the A-48 accelerator which was put into operation in 1954; it consisted of an ion injector operating at 100KV, and an Alvarez cavity about 12 feet in diameter and 20 feet in length. The proton output energy was 500Kev, and the operating efficiency over an eight-hour shift was 97%, with an output current of 220 mA. The highest rf gradient constantly maintained was 10% above the deuteron gradient; however, deuteron acceleration was not possible because the power supply of the injector could not provide the necessary 200 KV.

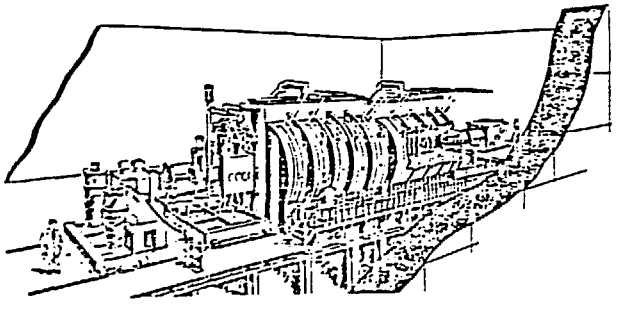

Fig. 1 Perspective drawing of A-48 accelerator.

Since 1952, W. B. Lewis,[2] working in Canada, has promoted the use of an accelerator for producing ^{233}U fuel to the closed fuel cycle of the CANDU reactor. Since the CANDU reactor, burning ^{233}U, has near-breeding characteristics (conversion ratio >0.9), a single 0.3A-1GeV accelerator breeder can supply fuel for about 12 reactors. In the 1960s, the Canadian concept evolved into the idea of an

Intense Neutron Generator[3] (or ING), which would have supplied an intense neutron source for research. However, the expense of this project would have consumed a large part of the budget allocated to scientific research in Canada, and such a redefinition of priority was not accepted.

Two decades after the MTA project, when the issue of non-proliferation of nuclear material was discussed in public debates, the concept of producing fissile material using an accelerator (accelerator breeder) was again raised and re-examined at Brookhaven National Laboratory (BNL).

To create a proliferation-resistant fuel cycle in a light-water reactor (LWR), we studied the so-called Linear Accelerator Fuel Regenerator (LAFR)[4] fuel cycle system. The main function of the cycle is to use spallation neutrons, which are produced by impinging medium energy protons (1-1.5GeV) into a liquid lead jet, to top up the initial fuel enrichment before burning, and also, to rejuvenate the burned or spent fuel discharged from the reactor to allow a second burn-cycle (see Fig. 2). Thus, LWR fuel assemblies that presently are enriched to 3% ^{235}U and burn to 30,000MWD/ton would yield 60,000 MWD/ton with an initial enrichment of only 2%. In this scenario, the LWR fuel assembly is detached without refabrication throughout the cycle. To achieve more burn up of the fuel, we also studied a second scenario in which the fuel burned in the first cycle is de-claded and refabricated without separating the fissile material from the fuel. In this case, reprocessing removes only the high-vapor-pressure fission product which has a poisoning effect on the second burning cycle.

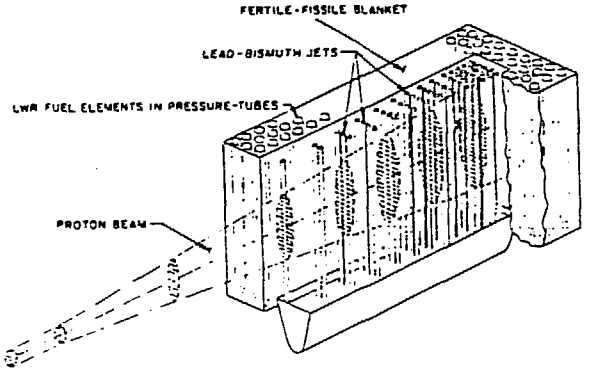

Fig. 2 Target-blanket configuration.

As was shown in an earlier neutron-yield experiment carried out by Fraser et al[5] (see Fig. 3), by injecting medium-energy protons directly into a fertile material, such as ^{238}U instead of lead, the neutron yield can be increased substantially; this, in turn,

results in a high rate of production of fissile material. When the Information Meeting on Accelerator Breeding was held at BNL in January, 1977,[6] the nuclear intra- and intercascade codes such as NMTC and HETC[7] did not have the capability of calculating the high energy fission reaction. The production rate of fissile material in the accelerator breeder was estimated from old experimental data[5] on neutron yields. By 1981, however, many authors[8] included the high-energy fission reactions in the nuclear cascade calculation. The newly developed codes were validated by comparing[9] them with the experimental results on neutron yield from large blocks of uranium carried out by Vasilikov[10], and with other experimental data.[5] Using these codes, we studied the concept of an accelerator breeder[11] in which medium-energy protons were impinged directly into the fertile material.

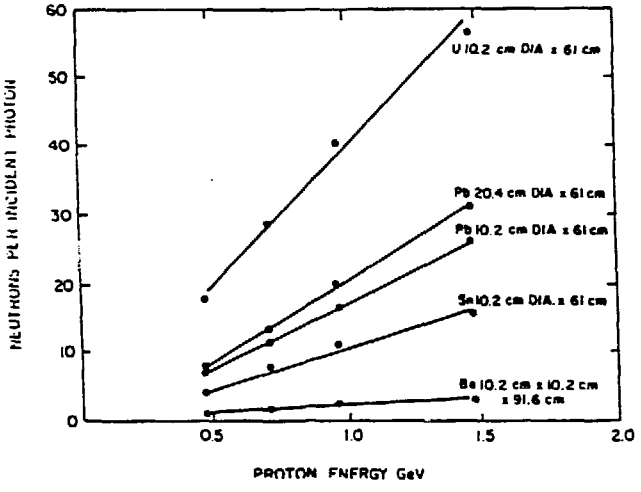

Fig. 3 Yield of neutrons obtained by bombarding a heavy metal target with medium energy protons (from Ref. 5).

The accelerator breeder facility consists of three main components: a) the accelerator; b) the target (Fig. 4); and c) the balance of the plant (BOP), which includes the steam

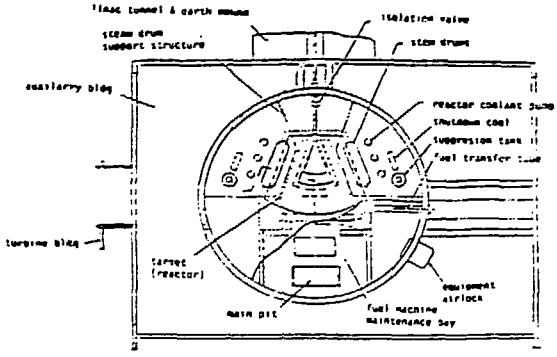

Fig. 4 The reactor containment building.

generator, turbine, and alternator. Table I gives the basic parameters of the proton linac. These parameters were chosen conservatively. The accelerator proton beam current of 300 mA CW was chosen as the maximum current; this current is far below the theoretical limits of space charge. The electrical efficiency of the accelerator is defined as the ratio of beam power to the feeding AC electric power. We estimated this efficiency to be 50% for 300mA linac,

Table I Parameters of Reference Concepts for the Accelerator Breeder.

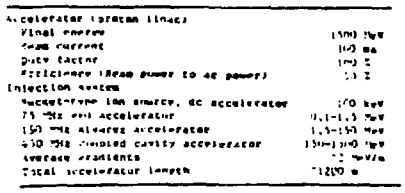

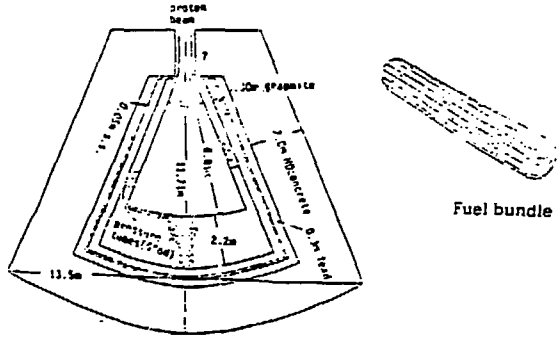

Fig. 5 Horizontal section through the reactor target.

assuming an rf power amplifier (klystron) with an efficiency of 70%. Figure 5 shows the target layout for the accelerator breeder and pressurized tubes. The size of target face (pressure tube assembly) is 3m x 5m and target depth is 2.2m. The entire assembly is contained in a "Hohlraum" pie-shaped vacuum vessel, lined with additional fuel material and a reflector to minimize the overall leakage of neutrons. To minimize the peak-power density and radiation damage, the 450 MW proton beam is defocused by a magnetic field; the front face of the target is almost uniformly bombarded by the proton beam, with a current density of about 2 $\mu A/cm^2$.

Table II shows the production rate of fissile fuel in the depleted uranium and thorium fuels (80% plant capacity), the amount of electricity generated, and the initial inventory of fissile materials in the target. For a depleted U (0.3% ^{235}U) or thorium target,

the electrical power generated is not sufficient to operate the accelerator.

Table II The Production Rate of Fissile Fuel, Generating Electric Power and the Initial Inventory of Materials.

Fuel	Coolant	Fissile fuel* (ton/year) production rate	Generated electric power (MW(e))	Initial fissile fuel inventory (ton)
UO_2 (^{235}U)	H_2O	1.66	340	3.3
	D_2O	1.83	450	3.3
U (^{235}U)	H_2O	2.61	780	0.55
	D_2O	2.71	690	0.55
Th	H_2O	1.81	285	0.0
	D_2O	1.82	270	0.0

*(plant factor 80%, 300 mA, 1.5 GeV proton beam).

In the case of UO_2 fuel, the fuel assemblies are similar to those used in the CANDU reactor; namely, the UO_2 fuel, cladded with zirconium, is inserted into zirconium pressure tubes. The fuel assemblies can be loaded, unloaded, and shuffled without interrupting the power operation. Heat is removed by H_2O (or D_2O) coolant in a single phase or in a boiling mode. A wide choice of materials and coolant/fuel ratio is allowed, because criticality of the target is not necessary. Therefore, a zirconium tube may not necessarily be the optimum choice; other materials, e.g. stainless steel, may ultimately prove more suitable.

By using a slightly enriched fuel, heat generation is substantially increased, and the electricity produced from this heat exceeds the electricity required to run the accelerator. However, the net (gain minus loss) production rate of fissile material does not change much in this neutron-moderated reactor, as shown in Table III. The table also shows data from a Na cooled and 6% ^{239}Pu fueled reactors which increase production rate of the fissile material.

Table III The Production Rate of Fissile Fuel Generating Electric Power and Initial Fissile-Fuel Inventory for UO_2 Enriched Fuel H_2O, D_2O, and Na-cooled Target Assembly.

Coolant	Enrichment	Fissile fuel (Pu) production rate* (ton/year)	Generating electric power MW	Inventory of fissile fuel ton
H_2O	^{235}U-3%	1.70	1033	3
	-6%	1.68	1578	6
	^{239}Pu-3%	1.65	1148	3
	-6%	1.71	1868	6
	-2+6%	1.65	1152	4
	-3+6%	1.66	1301	4.5
D_2O	^{235}U-3%	1.49	807	3
	-6%	1.67	1645	6
	-3+6%	1.56	965	4.5
Na	^{239}Pu-3%	1.39	972	2.5
	-6%	2.10	2768	5.0

*(plant factor-80%, 300 mA, 1.5 GeV proton beam).

III. ACTINIDE INCINERATOR

Studies have been made of the incineration of actinides in light-water reactors and in liquid metal fast breeders without processing the long-lived nuclei.[12] However, thermal neutrons and fast neutrons, whose spectrum is not sufficiently hard do not incinerate actinides efficiently. Incineration is inefficient because in these two types of reactor the neutron capture reaction, which creates another higher actinide, predominates over the fission reaction which incinerates the actinide. To incinerate the actinide, a fast reactor is required, which has a neutron spectrum hard enough to make the fission reaction dominate the capture reaction.

Mukaiyama et al[13] studied the following two types of fast reactors with higher actinide fuels. One type is the sodium-cooled bundle-pin type fuel with higher actinide alloyed with Zr and Y (BP-ABMR), and the other type is the He-cooled actinide burner-reactor with particle nitrate actinide fuel (PB-ABNR), which is similar to that used in the particle-fuel bed reactor at BNL[14].

In Figure 6, the core-averaged neutron spectra of the BP-ABMR inner core (Am-Cm-Y zone) and PB-ABNR are compared with those of the MOX fuel, LMFBR. The spectra of BP-ABMR and FBR are taken from the inner core. Table IV compares the ratio of fission rate to capture rate in various reactors; it is clear that the harder neutron spectrum of the BP-ABMR and PB-ABMR is necessary to incinerate the higher actinide.

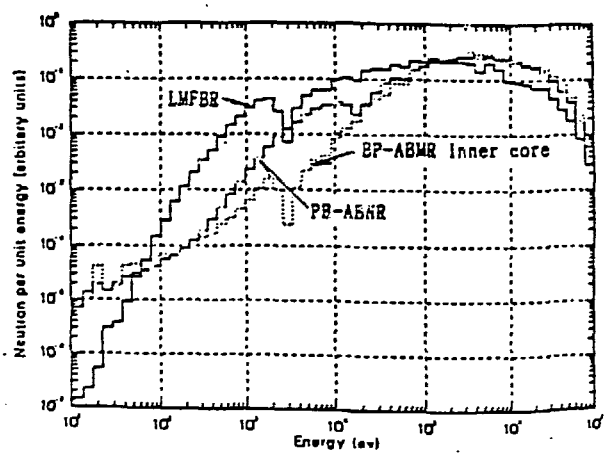

Fig. 6 Comparison of core-averaged neutron spectra in Mox fuel LMFBR, inner core of BP-ABMR, and PB-ABNR.

Table IV Comparison of the Ratios of Fission to Capture Rate.

Nuclide	PWR	FBR	BP-ABMR	PB-ABNR
^{237}Np	0.02	0.23	0.72[c]	0.64
^{238}Pu	0.08	1.43	2.7[c]	2.4
^{241}Am	0.01	0.19	0.68[b]	0.49
^{242m}Am	5.0	7.9	9.7[b]	8.9
^{243}Am	0.01	0.18	0.77[b]	0.52
^{242}Cm	0.25	1.0	3.8[b]	2.7
^{244}Cm	0.08	0.87	3.1[b]	2.2
E(Kev)[a] thermal		416	876[b], 761[c]	768

(a) : core averaged mean neutron energy
(b) : values in the inner core
(c) : values in the outer core

To evaluate the transmutation characteristics in detail, Mukaiyama et al calculated the burn-up for ^{237}Np, ^{241}Am, ^{243}Am, and ^{244}Am which were radiated in the constant flux for 400 days. The results of ^{237}Np and ^{243}Am are shown in Tables V (a) and (b). Their results show that in BP-ABMR and PB-ABNR, 20-30% of ^{237}Np is transmutated, half by fissioning and the other half by capture, while in PWR and FBR, ^{237}Np capture to the higher plutonium isotope predominates, fissioning of ^{243}Am in BP-ABMR and PB-ABNR is 12-14%, but only 3-4% in PWR and FBR, while in PWR, ^{23}Am capture to ^{244}Cm is 60%.

As demonstrated in Mukaiyama et al's detailed study, a much harder neutron spectrum is required to incinerate the higher actinide than is obtainable in the conventional LMFBR. However, the life time of neutrons in this harder spectrum is very short and the transient behavior of the reactor becomes more violent in the supercritical condition. To

Table V(a) Fraction of ^{237}Np Transmutated (α-decay half-life=2.14x10^6 year).

	PWR	FBR	BP-ABMR	PB-ABNR
Flux*	3.7	33	48	68
fissioned	3.0	4.7	9.5	14.2
capture to				
^{238}Np	0.2	0.1	0.1	0.1
^{238}Pu	24.1	13.9	9.7	13.8
^{239}Pu	2.7	0.6	0.4	0.9
^{240}Pu	0.4	0.01	0.01	0.02
^{241}Pu	0.3	0	0	0
^{242}Pu	0.03	0	0	0
sub total	27.7	14.6	10.2	14.8
transmuted	30.7	19.3	19.7	29.0
not transmuted	69.2	80.7	80.4	70.9
α-decay to ^{234}U	0.11	0.06	0.04	0.06

400 days irradiation
* Total Flux in 10^{14}n/cm^2·sec

obtain the hard neutron spectrum, the amount of the coolant in the reactor must be reduced, so that more stringent restrictions must be applied to operate this kind of reactor safely.

To keep the higher actinide fuel reactor running, the choices of the composite materials of fuel, cladding, structure, and coolant are very restricted: this makes the problem of safety associated with criticality much more severe. The accelerator actinide incinerator can resolve the difficulty in reactor safety, because it is a subcritical reactor, assisted by the neutrons created by the high-energy proton spallation and the high-energy fission reaction. The target

Table V(b) Fraction of ^{243}Am Transmutated (α-decay half-life=7950 years).

	PWR	FBR	BP-ABWR	PB-ABWR
Flux*	3.7	33	78	68
fissioned	3.8	3.4	14.2	11.8
capture to				
^{244}Am	0.03	0.02	0.02	0.02
^{244}Cm	59.1	22.2	28.2	28.7
Cm*	3.0	0.7	0.9	1.0
Pu*	0.6	0.02	0.04	0.04
^{241}Am	0.07	0	0	0
sub total	62.8	23.0	29.2	29.8
transmuted	66.6	26.3	43.4	41.6
not transmuted	32.8	73.2	56.0	57.9
α-decay to ^{239}Pu	0.7	0.5	0.6	0.6

400 days irradiation
\+ same as in TABLE
Pu* total of ^{238}Pu, ^{239}Pu, ^{241}Pu, ^{242}Pu, ^{244}Pu
Cm* total of ^{242}Cm, ^{245}Cm, ^{246}Cm

assembly is similar to that of the accelerator breeder that was discussed earlier, except that the fuel assembly is not depleted uranium but is actinide fuel.

Table VI shows the actinide waste from a 1000 MWe LWR after 33000 MWD/ton burn up which is processed with a 99.5% removal efficiency of uranium and plutonium. The neutron yield and the number of fissions in the interaction of the medium energy proton and higher

Table VI Actinide Waste from a Typical 1000 MWe LWR Reactor After Reprocessing.

Nuclide	Burn-up 1000 MWD_{th} (g)		Burn-up 3000 MWY (kg)
U-235	1.21		
236	0.618	144.83	not considered
238	143.0		
Np-237	23.1	23.1	18.97
Pu-238	0.025		
-239	0.815		
-240	0.327	1.374	1.13
-241	0.154		
-242	0.053		
Am-241	1.61	4.35	3.57
243	2.74		
Cm-242	0.177	0.271	0.22
-244	0.094		
		Sum	75.99

1) Reprocessing Plant Efficiency 99.5% for U and Pu

2) Plant factor: 75%

actinide nuclei is generally larger than that of the uranium nuclei. Figure 7 shows the neutron yields and the number of fissions when a proton is injected into infinite media of ^{237}Np and ^{238}U. The values are obtained from the NMTC-BNLF code,[8-4] which calculates the intra- and inter-nuclear cascade process, including high energy fissions.

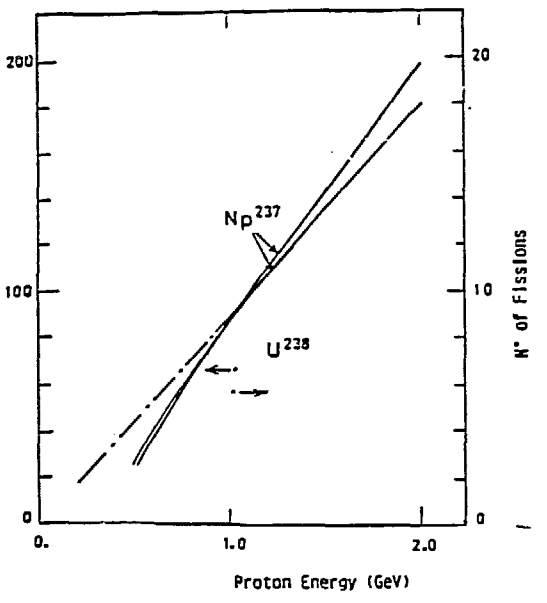

Fig. 7 Number of neutrons and number of fissions produced by high energy reactions in an infinite Np^{237} + U^{238} medium.

The study of mass distribution in the spallation process and high energy fission[15] shows that present cascade models do not create the mass between A = 20 ~ 30. A new mechanism in spallation has been studied.[16] To analyze the actinide incinerator in detail, especially to calculate the actinide burn-up, the neutron cross section of these actinides should be evaluated accurately.[17]

In transmuting the actinides[18], it would be unwise not to make use of the many fast neutrons coming from spallations, high energy fissions, and evaporation. Since these neutrons can induce further fissions in the target, they contribute substantially to the process of incineration.

In quantitative terms, the total number of fissions N_{fiss} can be expressed as:

$$N_{fiss} = N_h + S_h \frac{k}{\nu(1-k)} \qquad (1)$$

where N_h = total number of fissions due to high energy proton reactions, S_h = the number of neutrons produced by the high-energy proton reaction (spallation, high-energy fission, and evaporation) ν = number of neutrons per regular fission, and k = multiplication factor for regular fission.

The actinides produced annually from 10 units of 3000 MW(th) LWR without uranium isotopes is 246Kg, and the thermal power generated by incinerating this amount of actinide is 900MW. When this amount of actinide with the specific power of 150W/grHA is incinerated, the total inventory of actinide becomes 6 tons.

Our studies were carried out for systems cooled by sodium or helium. In both cases, the fuel pellets were assumed to consist of actinide oxides cladded by steel cans. The following design parameters were chosen (Table VI).

Table VII The Design Parameters

Pellet, outer diameter:	0.510 cm
SS clad, inner diameter:	0.524 cm
SS clad, outer diameter:	0.600 cm
Fuel Pitch:	0.75-0.85 cm
Active length:	80 cm

The target zone was surrounded by a thorium blanket in order to capture the large fraction of leakage neutrons to produce the fissile material of ^{233}U.

Table VIII shows the beam power requirements, the excess electricity produced, the effective multiplication factor, and the production rate of ^{233}U per year for both accelerator incinerators.

Table VIII Requirements for Accelerator-Driven Sodium- and Helium-Cooled Incinerators.

Coolant	K_{eff}	Beam Power (MW)	Beam Current 1GeV	3GeV	Reactor Power (MW_{th})	^{233}U Prod. in Blanket (kg)
Na	.90	27.9	27.9	9.3	900	85
He	.95	13.	13.	4.3	900	103

The first surprising result is the low beam-current required to incinerate the actinides produced by ten units of 1GWe LWRs. Depending on the beam energy (1 to 3 GeV) and the self-multiplication of the target, the required beam currents are between 5 ~ 15mA in the He-cooled incinerator, while in the sodium-cooled incinerator, this requirement would be raised by a factor of less than 2. A further reduction in proton beam current can be obtained by optimizing the fuel composition and the geometry of the target.

As a by-product, the actinide incinerator can produce annually at least 100Kg of fissionable material when the target is surrounded by a uranium or thorium blanket, and excess electricity of 240-270MW beyond the 30-60 MW required to operate the proton accelerator.

Takizuka et al[19] recently studied accelerator incinerators which are cooled by Pb-Bi or Na. The target geometry of these incinerators are close to that of our Linear Accelerator Fuel Generator except that they do not use a liquid lead target. The metallic actinide alloy fuel is employed, which provides a harder neutron spectrum than oxide fuel. The fuel assembly is similar to that of the LMFBR. Fuel pins with an active length of 100 cm are arrayed on a uniform triangular pitch. The pitches chosen for a Na and Pb cooled target are 8mm and 10mm, to keep the effective multiplication factors around 0.95. The geometric dimensions of the target assembly are shown in Figure 8.

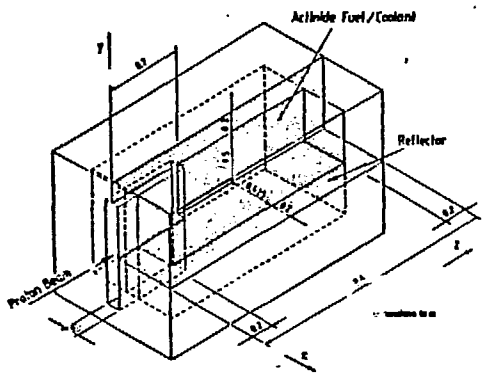

Fig. 8 Target design.

Due to the small area of the proton beam, the flux peaking factor is large, which limits the total power of incinerator and the incineration rate. The maximum power of a Pb-Bi cooled incinerator is lower than that of one that is cooled by Na. This difference is attributed mainly to the lower thermal conductivity of Pb-Bi.

Reduction of the flux peaking factor, which is important in increasing the incineration rate, can be achieved by using a target assembly with a large multiplication factor (k) and by reducing the leakage of neutrons from the target's surface. When the multiplication factor is less than 1, the flux has a sharp distribution and the fuel must be shuffled frequently. For this purpose, and also for maximizing heat removal, particle fuel, which is used in the design of high-flux research reactor, has many advantages over solid fuel. These advantages will be discussed in the next section.

To incinerate the actinide produced annually from 10 units of LWR, it is sufficient to use a medium-energy proton with a 15-30 mA current. Because of the nearly linear energy dependence of the number of spallation neutrons in the energy range 1-3 GeV, beam intensity and beam energy are exchangeable. These facts may favor the use of "multistage-parallel" cyclotrons over linear accelerators. While the price is almost proportional to energy for the latter, doubling or tripling the energy of a cyclotron is much less costly. On the other hand, the maximum achievable beam current of a cyclotron is rather limited, especially at low energies.

These considerations led to the concept of the so-called "multistage-parallel" cyclotron arrangement[14-2], consisting of a number of low-energy, low-current cyclotrons feeding into one high energy cyclotron.

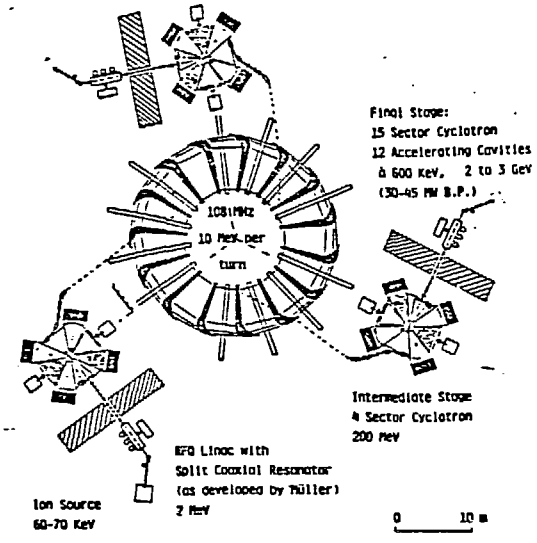

Fig. 9 Multistage cyclotron arrangement.

For example, (as shown in Fig. 9) a multistage cyclotron arrangement providing 15mA at an energy of at least 2 GeV would require the following assembly:

- three sources of 60-70 keV ions
- a low-energy 2 MeV, 5mA injector stage, consisting of three radiofrequency quadruple linacs (36 MHz) developed by Mueller from Darmstadt (Split Coaxial Resonator)
- an intermediate stage, made of the same number of four-sector cyclotrons with a phase width of 36° and frequency F_{Hf} = 36 MHz accelerating the 5mA proton current to an upper limit around 200 MeV
- a final-stage 15 sector cyclotron, fed by the three intermediate stages (3x5 mA at 200 MeV). This cyclotron works at 3x36=108 MHz using 12 acceleration cavities of 600 KeV. The final stage can reach a proton energy of 2 to 3 GeV at a beam power of 30-45 MW.

Before closing the discussion of accelerator breeders and actinide incinerators, it is worthwhile to mention other particle beams and their energies that have deuterons and tritons as the accelerated particles instead of protons.

The neutron yields from deuteron and triton injection are higher than the yields from protons in the low-energy regions. This difference is diminished at high energies above 3 GeV for deuterons, and above 5 GeV for triton.

One reason we chose protons over deuterons as the injected particles is because spilled deuterons produce neutrons when they collide with the accelerator's components, even in the low-energy range, which might contaminate an accelerator. If the technique of reducing beam loss in the low-energy accelerating region is improved so that contamination becomes less important, then using deuterons of 500-800MeV becomes more efficient than using protons of above 1GeV. Figure 10 shows that triton particles are more effective than deuteron particles.

As discussed above, a reduction in the leakage of neutrons from the target's surface is an important factor in achieving a high rate of production of fissile material and actinide incineration. Instead of lining the pie-shaped Hohlraum with additional fuel material, placing light-nuclei material, such as Li or Be, on the front surface of the target assembly will help reflect neutrons back from the surface.

When deuteron or triton are injected, the front material on the target assembly strips the neutrons from the injected particle, and makes the nuclear interaction more effective because there is no slowing down due to Coulomb interactions. These studies have not been made; they should be done to learn how to maximize the interaction between the high-energy particle beam and the target assembly.

The use of a much higher energy 1 TeV proton instead of a medium energy 1-2 GeV proton was studied by Wilson[20] He estimated the production rate of fissile material to be about half that of the medium-energy proton injection (1-3GeV) because many kinds of meson, baryon, and antibaryon production channels, are open at this high-energy range. Wilson's estimation was made with the old cascade code. It will be worthwhile to recalculate the production rate of fissile material using the improved cascade model codes to describe the high-energy nucleon-nucleus[21] and nucleus-nucleus reactions.[22]

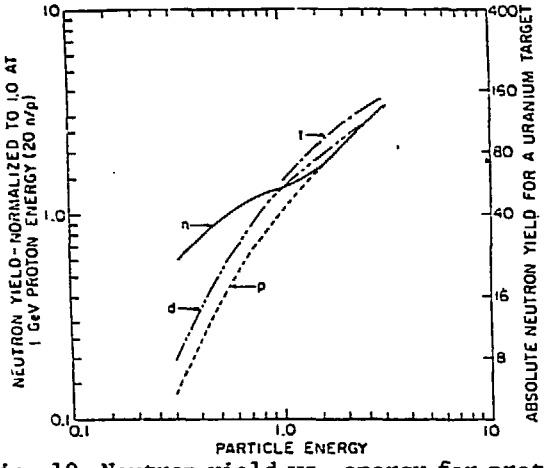

Fig. 10 Neutron yield vs. energy for proton, triton, deuteron, and neutron particles.

IV. PARTICLE FUEL

The distribution of neutron flux in the accelerator breeder and incinerator is steeper than that in the critical reactor because both the former are subcritical assemblies. This requires more frequent shuffling of the fuel, which is cumbersome for solid fuel. Particle fuel[19] is more suitable for this purpose.

A commercial type of burning HTGR particle fuel is composed of a central kernel of highly enriched fissile fuel (93.5% ^{235}U). The kernel can be uranium oxide, carbide, or oxy-carbide. Surrounding the fissile kernel is a porous layer of pyrographite, covered by several layers of pyrographite and silicon carbide. Fission product gases (krypton and xenon) collect in voids in the porous layer and kernel. The outer layers of the particle act as a miniature pressure vessel, holding all of the fission products (including the gases) inside the particle. The failure rate of such particle fuels is extremely low, about one in 10^4, even at very high burn-up (for example 50%) of the central kernel. (With more stringent quality control, the failure rate could be substantially reduced, possibly to one in 10^5).

In HTGRs, the burner particles are imbedded in large blocks or balls of graphite, which are then handled as the fuel elements. Heat generated in the particles flows out through the graphite blocks or balls to the coolant.

Particle fuel has an extremely large heat-transfer area in the packed bed (in the order of $100 cm^2 / cm^3$), and the small size (less than 1mm) of the particle fuel results in three

major benefits: 1. Very high power densities; 2. A small temperature difference between the fuel and coolant; and, 3. Minimum thermal stress and shock in the fuel. Thermal power densities in the packed bed can be 10MW/litre or more because of the large heat-transfer area.

Figure 11 shows a cycle of unloading and loading for a particle fuel element.

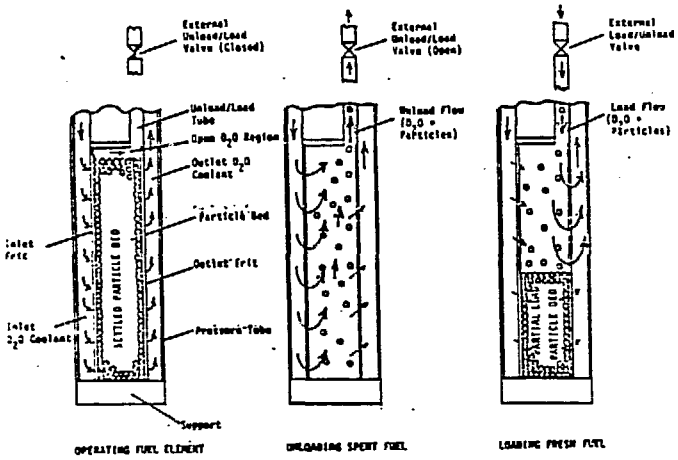

Fig. 11 Unload/load cycle for VHFR particle bed fuel element.

These advantages suggest that particle fuel might be suitable for the accelerator breeder and the accelerator incineration of actinides.

V. INCINERATION OF ^{137}Cs AND ^{90}Sr FISSION PRODUCTS

The ^{137}Cs and ^{90}Sr fission products both have a 30 year half-life: they are very difficult to incinerate in thermal neutrons because the cross sections of capture are 0.1 barn and 1 barn, respectively(note). To incinerate ^{137}Cs at 10 times the rate of natural decay, a thermal neutron flux of $10^{17}n/cm^2/sec$ is required; it is difficult to achieve such a high neutron flux in a fission reactor.

To incinerate these isotopes, Taube[24] proposed using the high thermal neutron flux created in the central D_2O-moderated region that is surrounded by molten salt-fast neutron regions. The scheme is shown in Figure 12.

To make one neutron which can be used for incinerating the fission product, the spallation reaction generates energy in the order of 10-20 MeV, which is less than the energy

generated by the fission reaction, namely 200MeV/(ν-1)~100MeV, where ν is the number of neutrons produced by a fission.

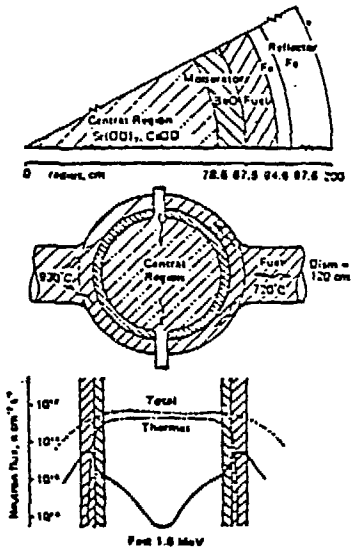

Fig. 12 Geometry of the high-flux burner reactor.

We studied the incineration of the fission products using the thermal neutron flux created by spallation neutron[25]. The scheme is very similar to the LAFR. The medium-energy protons are injected into the liquid Pb target, the spallation neutrons are thermalized in a surrounding assembly, which is composed of the ($^{137}Cs + D_2O$) and ($^{90}Sr + D_2O$) moderator. Figure 13 shows the geometrical parameters that we used. The heat generated by the spallation reaction is removed by the liquid lead jet; thus, a high neutron flux can be obtained. However, the thermal neutron cross-section of ^{137}Cs is so small that many of the thermal neutrons escape from the capture region, unless a large amount of ^{137}Cs is put into the region. However, from the safety point of view, it is not desirable to have a large inventory of ^{137}Cs and ^{90}Sr in the assembly: also, the incineration rate becomes low, as shown in Table IX.

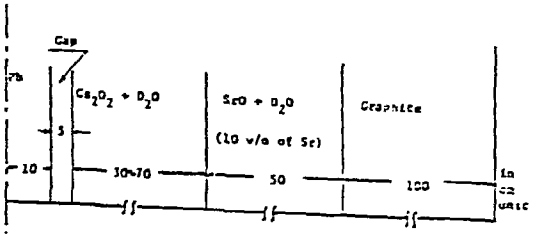

Fig. 13 System configuration of Table IX.

Table IX Effect of Cs_2O_2 Volume Fraction on Neutron Loss in Pb Target Region, Tr, Tn and Tv of ^{137}Cs and ^{90}Sr.

Zones				
Volume fraction of Cs_2O_2 in D_2O (v/o)		10	30	60
Total loading weight	$W(Cs_2O_2)$ (Kg)	0.45×10^3	2.24×10^3	3.58×10^3
W	W(SrO) (Kg)	0.47×10^3	0.47×10^3	0.47×10^3
Neutron loss in target region		0.49	0.34	0.24
Transmutation rate	^{137}Cs	$23.5 \lambda^{137}$	$11. \lambda^{137}$	$8.4 \lambda^{137}$
Tr ($sec.^{-1}$)	^{90}Sr	$24.8 \lambda^{90}$	$14.8 \lambda^{90}$	$14.5 \lambda^{90}$
No. of transmuted nuclei per	^{137}Cs	7.68	29.8	25.0
a proton, Tn (nuclei/proton)	^{90}Sr	13.01	19.1	8.52
Amounts of transmutation	Cs_2O_2	113	359	367
per year	(Cs)	(100)	(273)	(321)
Tv (Kg/year)	SrO	135	134	88
	(Sr)	(134)	(89)	(75.)

(note):
1. Section widths: $\delta Z(Cs) = \delta Z(Sr) = 90$, $Z_T = Z_E = 100$, in (cm).
2. Volume fractions: 1035 Pb, and 10 v/o SrO in Sm.
3. $\lambda^{137} = 7.33 \times 10^{-10}$, $\lambda^{90} = 7.82 \times 10^{-10}$, in ($sec.^{-1}$).

Another possible approach to creating high intensity neutrons would be to use muon catalyzed fusion reactions[26], if we can tailor the muon beam, (which is injected into a small synthesizer vessel) to a small beam-size and small momentum-spread.

We know that one muon causes 175 fusions in the liquid hydrogen density dt target; these numerous fusions occur in a very limited region of the target. at the point where the muons are halted. Therefore, if we could stop a large number of muons in a very small region, the fusion neutron intensity would become extremely high.

The 14MeV neutrons produced by the (dt) fission reaction has a 1-2 barn cross-section for (n,2n) and (n,3n) reaction in both ^{137}Cs and ^{90}Sr isotopes. Thus, the 14MeV fusion neutron flux of $10^{16} n/cm^2/sec$ can incinerate these isotopes with a rate that is 10 times that of natural decay. However, a Tokomak-type fusion reactor cannot produce such a high neutron flux in the first wall region. Although the inertial fusion device can create a much higher neutron flux in the dt target regions, it requires a more complicated design in which the dt fuel pellet is combined with the fusion products.

The heat deposition of this reaction is caused mostly by stopping the 3.1MeV α particle created by the dt fusion reaction. Also, a few of the 14MeV neutrons deposit their heat as they are slowed down in the small synthesizer. Thus, the heat deposition to create one 14MeV is smaller than in spallation or fission reactions.

The economics of producing one 14MeV neutron by the muon-catalyzed fission reaction, taking into account the energy cost of producing 14MeV neutrons, is 4.5GeV/175 ≈ 26MeV, a value which is comparable to that of producing spallation neutrons.

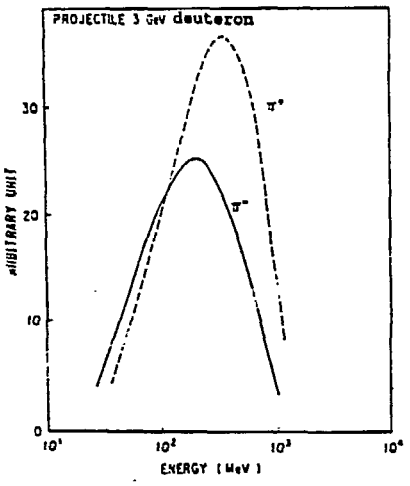

Fig. 14 Energy spectra of π^- and π^+ mesons emitted from Be target.

The synthesizer designed by Petrov[27] for muon-catalyzed fusion has an extremely long length of 20m, because of the momentum spread of π^- created by impinging medium energy protons of 3GeV into a light nuclei target, such as Be. Figure 14 shows the longitudinal momentum distribution of π^- mesons. Therefore, the range of the μ^- created by the decay of π^- in the liquid hydrogen density dt mixture is widely spread (20m).

A reduction in the spread of μ^- momentum might be accomplished in the following way. First, by separating out π^- particles with different momenta by a magnetic field, and also by slowing down the transformed μ^- from the π^- of different sizes in a slowing-down medium, as shown in Figure 15.

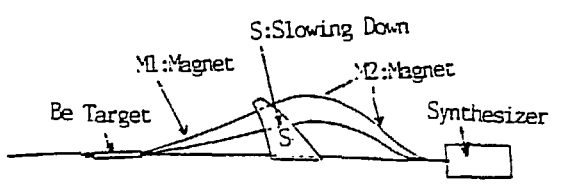

Fig. 15 Tailoring of π^- and μ^- particles.

Second, by reducing the spread of the μ^- momentum, the μ^- beam, in which energy is still high, can penetrate the window of the synthesizer vessel. Third, some further

reduction of energy can be achieved using a D_2O medium, in which the slowing-down power is about 16 times larger than in a D-T mixture.

Figure 16 shows the conceptual design of a dt MuCF neutron source reactor. The μ^- beam is created by injecting a 4GeV 5 mA current deuteron into a Be target. The π^-, and its decay product μ^-, are tailored to a small momentum spread before entering the synthesizer that has a 4cm diameter.

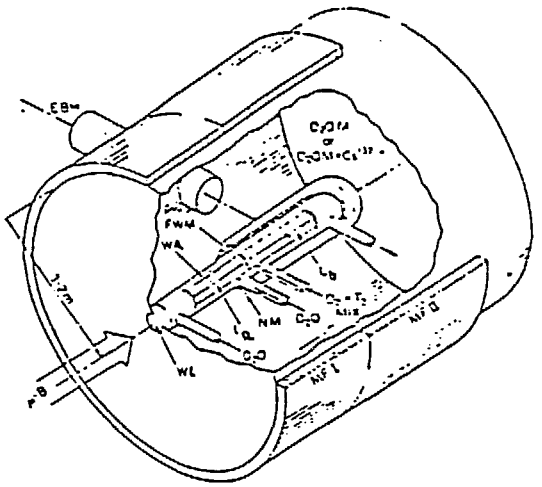

E.B.H.:	Experimental Beam Hole
F.W.M.:	First Wall Material for Magnetic Fusion Reactor (Thickness 10cm)
MFI:	Magnetic Field for μ^- Energy Control
MFII:	Magnetic Field for Stopped μ^- Distribution Control
N.M.:	Neutron Multiplier of Be (20 thickness) or Pb (3cm Thickness)
D_2OM:	D_2O Moderator for Thermalizing Neutron
D_2OM+Cs^{137}:	D_2O Moderator for Increasing Cs-137 by (α, γ) Reaction
M.B:	μ^- Beam Dia. 3–4cm 3.6 mA
l_a:	Length of D_2O Section 50cm–100cm
l_b:	Length of D_2T_2 Mixture Section 34cm
WT:	μ^- Beam Window (High Stress S.S.) Thickness ~1cm
WA:	Wall of Synthesizer (High Stress S.S.)

Fig. 16 Fusion high-intensity neutron source reactor: DT muon catalyzed.

The synthesizer contains D_2O at 1000 atm pressure (for slowing down the energy) and dt mixture. When a 3.6mA μ^- beam, with an energy of 200MeV penetrates the 1cm-thick window of the synthesizer, the heat deposited in the window is 10KW, which can be removed by the D_2O coolant surrounding the window. Since each μ that is stopped in the dt region produces 175 fusions, the total number of fusion per sec is 3.8×10^{18}/sec, and the heat production due to the 3.5MeV alpha particle is 1.1MW. By circulating the dt mixture to an outside heat exchanger, 5MW per liter heat production can be removed. Choosing a volume of the heat-producing DT region of about 0.44 litre, the length of the fusion-reaction zone becomes 34cm. The 14MeV neutron flux at the surface of the reacting target region then is 9×10^{15}/sec/cm^2, and, thus, these neutrons can

be used to incinerate ^{137}Cs and ^{90}Sr, for a testing of the first material of the Tokomak wall, or for treating the thermal neutron source by multiplying the number of neutrons using a multiplying medium, such as Be and Pb.

Another approach that has been studied for incinerating ^{137}Cs and ^{90}Sr by γ-rays is the large giant resonance (γ,n) reaction.[28] The giant resonance cross-section of the (γ,n) reaction for these isotopes are of the order of 500mb, so that the high intensity γ-ray created by injecting a high-intensity electron beam into a target composed of the fission products can incinerate them at a high rate. However, other reactions, such as pair productions due to nuclear and electron fields, and incoherent scattering becomes larger than the (γ,n) reaction. Thus, most of the γ-rays are lost in these reactions before incineration occurs.

The giant dipole resonance is composed of a collection of many small resonances which have a high cross-section and small width. At the energy range near neutron binding, the width becomes of the order of an ev. Some of the (γ,n) resonance cross-section might be higher than the reaction of pair production and incoherent scattering. Therefore, if we can make a high intensity γ-ray, with an energy close to that of neutron-binding energy and with a very small energy width the order of an ev, the incineration of ^{137}Cs and ^{90}Sr might be feasible.

It might be possible to generate such a high intensity γ-ray laser by using the coherent γ-ray emission in a stimulated annihilation of a highly focused electron-positron pair. Bertollitti et al[29] formulated the critical pair density Nc for stimulating annihilation as:

$$N_c = \frac{4 \times 10^{20}}{n_f} \text{ cm}^{-3} \qquad (3)$$

where n_f is the number of photons in each polarization per mode.

The Stanford Linear Collider can focus electron and positron beam to the order of a few microns. The number of electrons in one bucket is 5×10^{12}, and the length of the bucket is a few cm, so that density of the electron in the colliding region is about $5 \times 10^{12}/\text{cm}^3$. Based on this data, a coherent γ-ray

emission in a stimulated e-$\bar{e}$ pair annihilation can be achieved by $n_t = 10^2$. For our purpose, to make such an γ-ray laser with an energy of about 7 MeV requires the acceleration of an electron and positron of 6.5MeV.

VI. FUTURE ACCELERATOR TECHNOLOGY

Present-day accelerator technology uses microwaves, which were developed before WWII, to accelerate charged particles. To accelerate a 1GeV proton, Linac must be about 0.8Km in length.

Although the development of exotic ideas, such as plasma beat waves[30] and wake fields[31], which stirred up excitement a few years ago, have not materialized, these kinds of approaches are the next step in the development of accelerator technology.

Laser technology is advancing with astonishing speed. The laser power needed to create an electric field of 1GV/m is 6.8×10^{18} watt/cm^2, and the beam can be focussed so that it is only microns in size. Practically, the laser power needed to accelerate a charged particle with an acceleration of 1 GeV/m would be of the order of 1 Kw.

At BNL, Palmer et al[32] are studying the acceleration of charged particles using the electric field created by irradiating a CO_2 laser onto a miniature grated lattice. (See Fig. 16). This approach might be useful for tailoring the momentum distribution of particles such as $\mu^{\pm}$ and antiprotons[1] that are produced by injecting high-energy protons into a long, thin target whose grated surface is irradiated by the laser.

---

[1]Only a very small fraction, of 10^{-5}, is collected from the antiprotons produced by impinging the 120 GeV proton onto a copper target; only the antiprotons which fall in the momentum bucket of the storage ring can be captured. By reducing the momentum spread of the antiprotons, the efficiency of capture can be increased. These antiprotons[23] are used for elementary particle studies, to search for antigravity, for medical application, and for fuel for a future deep-space exploration rocket.

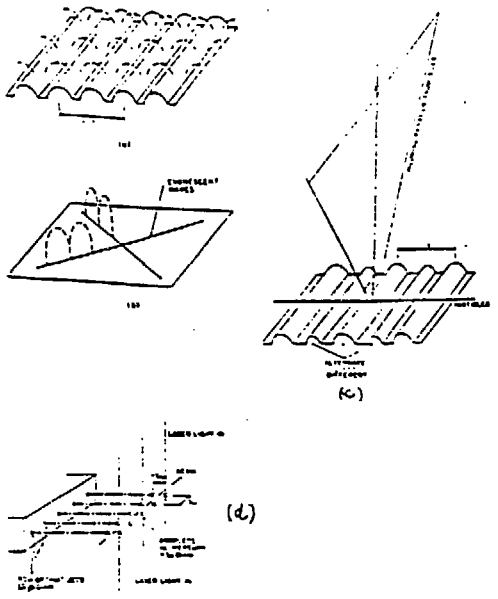

Fig. 17 a) Field over a Resonating Grating.
b) Components of Fields.
c) Modified Grating Coupling to Incoming Radiation.
d) Droplet Accelerator Concept.

A more exotic approach[31] to acceleration is the proposal to channel particles in single crystal, as the accelerating cavity. The electric field created by exciting the electron density wave by laser would be used to accelerate the charged particle.

Theoretical studies of the interaction of the channeled relativistic electron and the electron density wave in a single crystal under the laser irradiation is a very challenging problem. This problem might be solved with an approach similar to that used for studying the free electron laser[33]. The theory might be useful in the future design of a single crystal window, through which a well aligned charged particle would pass with less collisions than through a regular window.

ACKNOWLEDGEMENT

The author would like to express his thanks to Drs. H. Kouts, J. Powell, M. Steinberg, P. Grand, Y. Nakahara, and N. Mizoo for many useful discussions and Dr. Woodhead for the editorial work. This work was performed under the auspices of the U.S. Department of Energy under Contract No. DE-AC02-76CH00016.

REFERENCES

(1-1) C. Van Atta, J. Lee, W. Heckrott, Lawrence Livermore Laboratory, UCRL-52144 (1976).

(1-2) C. Van Atta, Lawrence Livermore Laboratory, UCRL-79151, (1977).

(1-3) C.M. Van Atta, "A Brief History of the MTA Project"; Ref. (6), P.20, (1977) Jan 18-19.

(2-2) W. Lewis, Atomic Energy of Canada Ltd., Rapport AECL-969, (1953).

(2-2) S.O. Schriever, "Canadian Accelerator Breeder System Development"; Rapport AECL-7840, (1982).

(3) W. Lewis, Atomic Energy of Canada, Ltd., Rapport AECL-3190, (1968).

(4) P. Grand, H. Kouts, J. Powell, M. Steinberg, H. Takahashi; "Conceptual Design and Economical Analysis of Light Water Reactor Fuel Enrichment/Regenerator", BNL 50838, (UC-80, TID-4500), (1978).

(5) J. Fraser, Green, Hilborn, Milton, Gibson, Gross, Zucker, #AED-Conf. Report 65-288-9.

(6) H. Kouts, M. Steinberg (ed), Proc. Inform Meeting, Accelerator-Breeding, Jan. 1977. BNL, Report Conf. 770107, (1977).

(7) Radiation Shielding Information Center, ORNL, "NMTC Monte Carlo Nucleon-Meson Transport Code" CCC-161, "Monte Carlo High-Energy Nucleon-Meson Transport Code CCC-178."

(8-1) F. Alsmiller, et.al., Bull. of American Phys. Soc., 24, (1979), 874.

(8-2) F. Atchinson, Private Communication.

(8-3) Y. Nakahara, T.Tsutsui JAERI Memorandum M82-198.(1982).

(8-4) H. Takahashi, Symposium on Nuclear Cross Section from 10-50 MeV; "Fission Reaction in High Energy Proton Cascade"; Brookhaven National Laboratory, May 12-14, (1980), BNL-NCS-51245.

(8-5) P. Fong, "Statistical Theory of Nuclear Fission", New York: Gordon & Breach, 1969.

(9) Y. Nakahara, H. Takahashi; Atomnaya Energina, 47, (1979), 83.

(10-1)R.G. Vasil'kov et al., "Mean Number of Secondary Neutron by High Energy Proton" Yadern. Fiz. 7, 88, (1968), Trans: Sov. J. Nucl. Phys. 7, 64, (1968).

(10-2)R.G. Vasil'kov, V.I. Goldanskii, et. al.; Atomnaya Energiya 46, (1978), 329.

(11-1) Takahashi, J. Powell, and H. Kouts; "Accelerator Breeder with Uranium and Thorium Target"; Atomkernenergie - Kerntechnik, 44, 181, (1984).

(11-2)F.R.Maynatt, Ref. 6, P.85.

(11-3)K.D.Larthrop and J.C.Vigil, Ref. 6, P.177.

(11-4)K. Furukawa, K. Tsukada, Y. Nakahara; "Molten-Falt Target and Blanket Concept, Inter-collaboration on Advanced Neutron Source, ICAN-S-N, Oct. 20-24, 1980; KEK, Tsukuba.

(12) Int. Conf. on Nuclear Waste Transmutation, July 22-24, 1980, Austin, Texas.

(13) T. Mukaiyama, H. Takano, T. Takizuka, T. Ogawa, and M. Osakabe; "Conceptual Study of Actinide Burner Reactor"; Proc. 1988, Int. Reactor Physics Conference, (Jackson Hole 1988).

(15) T. Nishida, H. Takada, I. Kanno, Y. Nakahara, Computer Process & Nuclear Data Needs for the Analysis of Actinide Transmutation by a Particle Accelerator, Report on OECD NEA Data Bank Meeting (12-13 Dec. 1989).

(16) Y. Nakahara and H. Takada. Private communication.

(17-1)H. Takano and K. Kaneko; "Revision of Fast Reactor Growth Constant Set"; JFS-3-J2. JAERI-Memorandum-M89-141; (1989, Oct.).

(17-2)H. Takano, T. Mukaiyama, et.al.; JAERI-M-89-072, (1989, June).

(18-1)H. Takahashi; "Actinide Transmutation by the Spallation Process"; Workshop on the Feasibility of Research Program on Actinide Transmutation by Spallation Process, Ispira, June 21, (1985). EURATOM Memorandum.

(18-2)P. Bonnaue, H. Rief, P. Mandrillon, and H. Takahashi; "Actinide Transmutation by Spallation in the Light of Recent Cyclotron Development"; NEACRP-A-910, Session B.1.2, (1987). (European American) Reactor Physics Committee Report.

(19) T. Takizuka, I, Kanno, H. Takada, T. Ogawa, T. Nishida, and Y. Kaneko; "A Study on Incineration Target System"; International Conference on Emerging Nuclear Energy"; held at Kalrsruhe, July 3-7, (1989).

(20) R. Wilson (Fermi Lab), Private communication.

(21) B. Anderson, G. Gustafson, and B. Nielsson, Almquist Nucl. Phys. B281, 289 (1987).

(22) K. Werner, Phys. Letter, 197B, 225 (1987).

(23-1)J. Powell and H. Takahashi; "Very High Flux Research Reactors Based on Particle Fuel"; IAEA-CN-48/038; International Conference on Neutron Scattering in the '90s.

(23-2)J. Powell and F. Horn; "High Power Density Reactors Based on Direct Cooled Particle Bed"; Space Nuclear Power System, 319, (1985).

(24) M. Taube; "The Transmutation of Sr^{90} and Cs^{137} in a High Flux Fast Reactor with a Thermalized Central Region"; Nucl. Sci-Eng., 61, 212, (1976).

(25) H. Takahashi, N. Mizoo, and M. Steinberg; "Use of the Linear Accelerator for Incinerating the Fission Product of Cs^{137} and Sr^{90}"; International Conference on Nuclear Waste Transmutation, July 22-24, 1980. The University of Texas at Austin.

(26-1)H. Takahashi, et.al.; "Nuclear Fuel Breeding by Using Spallation and Muon Catalyzed Fusion Reaction; Atomkernenergie, Kerntechnik; 36, 195, (1980).

(26-2)H. Takahashi, "Muon Catalyzed Fusion in Plasma State and High Intensity DT Fusion Neutron Source"; International Conference on Emerging Nuclear Energy held at Kalrsruhe, July 3-7, (1989).

(27) Yu. Petrov, Muon Catalyzed Fusion 1, 351 (1987), 3, 525 (1988).

(28) T. Matsumoto, Nucl. Instr. Method A268,234 (1988).

(29) M. Bertoletti and C. Sibilia, "Coherent γ-Emission by Stimulated Annihilation of Electron-Positron Pair. App. Phys., 19, 127-130, (197-9).

(30) T. Tajima and J. M. Dawson, PRL, 43 267 (1979).

(31) B. Newberger, "Laser Plasma Interaction and Particle Acceleration," U.S. Particle Accelerator School, BNL, 24 July - 4 Aug. (1988).

(32) Proc. Workshop Laser Acceleration of Particle, Malibu, CA (1985), AIP #130.

(33) H. Takahashi, "Theory of Free Electron Laser", Physica 123, 225 (1984).

(34) B. Augenstein, B. Bonner, F. Mills, and M. Nieto; "Proceeding of the Rand Workshop on Antiproton Science and Technology"; The Rand Corporation, U.S.A., Oct. 6-9, 1987, World Scientific.

Note

The author was informed at this symposium that the thermal neutron capture cross section of ^{137}Cs was measured as 0.25~0.26[1] barns (preliminary estimation) by a Japanese group[1], instead of 0.11 barns[2], and the recent evaluated thermal neutron capture cross section of ^{90}Sr is 14m barns[2] instead of 1 barn used in the calculation. The data cited in the text are old, and these cross sections are not well established yet. They should be re-measured and re-evaluated for study for fission product incineration.

(1) H. Harada, et.al., "Study of Transmutation for F.P.(1) Thermal Neutron Capture Cross Section of the Reaction $^{137}Cs(n,\gamma)\ ^{138}Cs$", to be published, (1990).

(2) F.W. Walker, et.al., "Chart of the Nuclides", 14 Edition, Knoll Atomic Power Laboratory, (1988).